Persistent Entropy for Separating Topological Features from Noise in Vietoris-Rips Complexes *

Nieves Atienza¹, Rocio Gonzalez-Diaz¹, Matteo Rucco²

Depto. Mat. Aplic. I, E.T.S.I. Informatica,
 University of Seville, Spain
 email: {natienza,rogodi}@us.es
 School of Science and Tech., Computer Science Division,
 University of Camerino, Italy
 email: matteo.rucco@unicam.it

January 30, 2017

Abstract

Persistent homology studies the evolution of k-dimensional holes along a nested sequence of simplicial complexes (called a filtration). The set of bars (i.e. intervals) representing birth and death times of k-dimensional holes along such sequence is called the persistence barcode. k-Dimensional holes with short lifetimes are informally considered to be "topological noise", and those with long lifetimes are considered to be "topological features" associated to the filtration. Persistent entropy is defined as the Shannon entropy of the persistence barcode of a given filtration. In this paper we present new important properties of persistent entropy of Čech and Vietoris-Rips filtrations. Among the properties, we put a focus on the stability theorem that allows to use persistent entropy for comparing persistence barcodes. Later, we derive a simple method for separating topological noise from features in Vietoris-Rips filtrations.

Keywords: Persistent homology, persistence barcodes, Shannon entropy, \check{C} ech and Vietoris-Rips complexes, topological noise, topological feature

1 Introduction

Topology is the branch of mathematics that studies shapes and maps among them. From the algebraic definition of topology a new set of algorithms have

 $^{^{*}\}mathrm{Authors}$ are partially supported by Spanish Government under grant MTM2015-67072-P (MINECO/FEDER, UE).

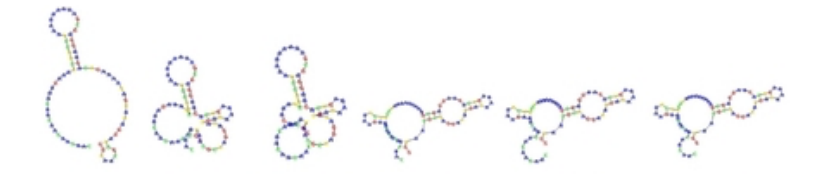


Figure 1: From left to right: RNA secondary suboptimal structures within different bacteria.

been derived. These algorithms are identified with "computational topology" or often pointed out as Topological Data Analysis (TDA) and are used for investigating high-dimensional data in a quantitative manner.

Persistent homology appears as a fundamental tool in Topological Data Analysis. It studies the evolution of k-dimensional holes along a sequence F of simplicial complexes. The persistence barcode B(F) of F is the collection of bars (i.e. intervals) representing birth and death times of k-dimensional holes along such sequence. In B(F), k-dimensional holes with short lifetimes are informally considered to be "topological noise", and those with long lifetimes are "topological features" of the given data.

Persistent homology based techniques are nowadays widely used for analyzing high dimensional data-set and they are good tools for shaping these data-set and for understanding the meaning of the shapes. Persistent homology reveals the global structure of a data-set and it is a powerful tool for dealing with high dimensional data-set without performing dimensionality reduction. There are several techniques for building a topological space from the data. The main approach is to complete the data to a collection of combinatorial objects, i.e. simplices. A nested collection of simplices forms a simplicial complex. Simplicial complexes can be obtained from graphs and point cloud data (PCD) [1, 2]. For example, PCD can be completed to simplicial complexes by using the Vietoris-Rips filtration, which is a sequence of simplicial complexes built on a metric space, providing in this way a topological structure to an otherwise disconnected set of points. It is widely used in TDA because it encodes useful information about the topology of the underlying metric space. Let us take a look at Fig. 1, it represents a collection of RNA secondary sub-optimal structures within different bacteria. All the shapes are characterized by several circular substructures, each of them is obtained by linking different nucleotides. Each substructure encodes functional properties of the bacteria. Mamuye et al. [3] used Vietoris-Rips complexes and persistent homology for certifying that there are different species but characterized with the same RNA sub-optimal secondary structure, thus these species are functionally equivalent. The mathematical details of Vietoris-Rips filtration are given in Section 2 of this paper.

Nevertheless, Vietoris-Rips based analysis suffers of the selection of the parameter ϵ . Generally speaking, for different ϵ , different topological features can be observed. For example, in [4], several applications of Vietoris-Rips based analysis to biological problems have been reported and examples of different ϵ

with different meaning were found. In order to select the best ϵ , some statistics have been provided what is known as "persistence landscape" [5]. Landscape is a powerful tool for statistically assessing the global shape of the data over different ϵ . Technically speaking, a landscape is a piecewise linear function that basically maps a point within a persistent diagram (or barcode) to a point in which the x-coordinate is the average parameter value over which the feature exists, and the y-coordinate is the half-life of the feature. Landscape analysis allows to identify topological features. In Section 6, we present the notion of persistent entropy, as an alternative approach to landscape. The main difference between landscape and our method is that the former uses the average of ϵ , while the latter works directly on fixed ϵ . More concretely, persistent entropy (which is the Shannon entropy of the persistence barcode) is a tool formally defined in [6] and used to measure similarities between two persistence barcodes. A precursor of this definition was given in [7] to measure how different the bars of a barcode are in length. In [8], persistent entropy is used for addressing the comparison between discrete piecewise linear functions. In Section 11, several properties of the persistent entropy of Vietoris-rips filtrations are presented. For example, the exact formula of maximum and minimum persistent entropy is given for a persistence barcode, fixing the number of bars and the maximum and minimum length. These results are important later in Section 15 for differentiate topological features from noise.

In general, "very" long living bars (long lifetime) are considered topological features since they are stable to "small" changes in the filtration. In [9] a methodology is presented for deriving confidence sets for persistence diagrams to separate topological noise from topological features. The authors focused on simple, synthetic examples as proof of concept. Their methods have a simple visualization: one only needs to add a band around the diagonal of the persistence diagram. Points in the band are consistent with being noise. The first three methods in that paper were based on the distance function to the data. They started with a sample from a distribution \mathbb{P} supported on a topological space \mathfrak{C} . The bottleneck distance was used as a metric on the space of persistence diagrams. The last method in that paper used density estimation. The advantage of the former was that it is more directly connected to the raw data. The advantage of the latter was that it is less fragile; that is, it is more robust to noise and outliers. In Section 15 in this paper, we derive a simple method for separating topological features from noise of a given filtration using the mentioned persistent entropy measurement. Moreover, we claim it is very easy (and fast) to compute, and easy to adapt depending on the application. A preliminary version of this technique was also presented in [10].

2 Background

This section provides a short recapitulation of the basic concepts needed as a basis for the presented method for separating topological noise from features.

Informally, a topological space is a set of points each of them equipped with

the notion of neighboring. A simplicial complex is a kind of topological space constructed by the union of k-dimensional simple pieces in such a way that the common intersection of two pieces are lower-dimensional pieces of the same kind. More concretely, K is composed by a set K_0 of 0-simplices (also called vertices V, that can be thought as points in \mathbb{R}^d); and, for each $k \geq 1$, a set K_k of k-simplices $\sigma = \{v_0, v_1, \ldots, v_k\}$, where $v_i \in V$ for all $i \in \{0, \ldots, k\}$, satisfying that:

- each k-simplex has k+1 faces obtained by removing one of its vertices;
- if a simplex is in K, then all its faces must be in K.

The underlying topological space of K is the union of the geometric realization of its simplices: points for 0-simplices, line segments for 1-simplices, filled triangles for 2-simplices, filled tetrahedra for 3-simplices and their k-dimensional counterparts for k-simplices. We only consider finite simplicial complexes with finite dimension, i.e., there exists an integer m (called the dimension of K) such that for k > m, $K_k = \emptyset$ and, for $0 \le k \le m$, K_k is a finite set.

Two classical examples of simplicial complexes are Čech complexes and Vietoris-Rips complexes (see [11, Chapter III]). Let V be a (finite) PCD in \mathbb{R}^d . The Čech complex of V and r denoted by $\check{C}_V(r)$ is the simplicial complex whose simplices are formed as follows. For each subset S of points in V, form a closed ball of radius r around each point in S, and include S as a simplex of $\check{C}_V(r)$ if there is a common point contained in all of the balls in S. This structure satisfies the definition of abstract simplicial complex. The Vietoris-Rips complex denoted as $VR_V(r)$ is essentially the same as the Čech complex. Instead of checking if there is a common point contained in the intersection of the (r)-ball around v for all v in S, we may just check pairs adding S as a simplex of $\check{C}_V(r)$ if all the balls have pairwise intersections. We have $\check{C}_V(r) \subseteq VR_V(r) \subseteq \check{C}_V(\sqrt{2}r)$. See Fig.2. In practice, Vietoris-Rips complexes are more often used since they are easier to compute than \check{C} ech omplexes.

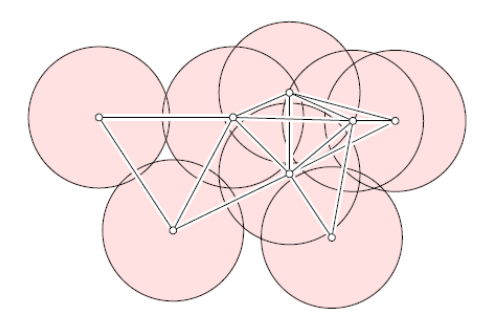


Figure 2: [11, p. 72] Nine points with pairwise intersections among the disks indicated by straight edges connecting their centers, for a fixed time ϵ . The Čech complex $\check{C}_V(\epsilon)$ fills nine of the ten possible triangles as well as the two tetrahedra. The Vietoris-Rips complex $VR_V(\epsilon)$ fills the ten triangles and the two tetrahedra.

Persistent homology is a method for computing k-dimensional holes of a given topological space at different spatial resolutions. The key idea is as follows.

- \bullet First, the space must be represented as a simplicial complex K and a distance function must be defined on the space.
- Second, a filtration of K, referred above as different spatial resolutions, is computed. More concretely, a filtration F of K is a collection of simplicial complexes $F = \{K(t) | t \in \mathbb{R}\}$ of K such that $K(t) \subset K_s$ for t < s and there exists $t_{\text{max}} \in \mathbb{R}$ such that $K_{t_{\text{max}}} = K$. The filtration time (or filter value) of a simplex $\sigma \in K$ is the smallest t such that $\sigma \in K(t)$. For example, let V be a PCD in \mathbb{R}^d and let $r, r' \in \mathbb{R}$. Then, there is a natural inclusions $\check{C}_V(r) \subseteq \check{C}_V(r')$ and $VR_V(r) \subseteq VR_V(r')$ whenever $r \leq r'$. The simplicial complexes $\check{C}_V(r)$ together with the inclusion maps define a filtered simplicial complex $VR_V(r)$ together with the inclusion maps define a filtered simplicial complex $VR_V(r)$ together with the inclusion maps define a filtered simplicial complex $VR_V(r)$ together with the inclusion maps define a filtered simplicial complex $VR_V(r)$ together with the inclusion maps define
- Then, persistent homology describes how the homology of a given simplicial complex K changes along filtration $F = \{K(t) | t \in \mathbb{R}\}$. If the same topological feature (i.e., k-dimensional hole) is detected along a large number of subsets in the filtration, then it is likely to represent a true feature of the underlying space, rather than artifacts of sampling, noise, or particular choice of parameters. More concretely, a bar in the k-dimensional persistence barcode, with endpoints $[t_{start}, t_{end})$, corresponds to a k-dimensional hole that appears at filtration time t_{start} and remains until filtration time t_{end} . The set of bars $[t_{start}, t_{end})$ representing birth and death times of homology classes is called the persistence barcode B(F) of the filtration F. Analogously, the set of points $(t_{start}, t_{end}) \in \mathbb{R}^2$ is called the persistence diagram dgm(F) of the filtration F.

For more details and a more formal description we refer to [11].

Classically, the bottleneck distance (see [11, page 229]) is used to compare the persistence diagrams of two different filtrations. Concretely, let $dgm(F) = \{a_1, \ldots, a_k\}$ and $dgm(F') = \{a'_1, \ldots, a'_{k'}\}$ be, respectively, the persistence diagram dgm(F) and dgm(F') of the two filtrations F and F', then

$$d_b(dgm(F), dgm(F')) = \inf_{\gamma} \{ \sup_{v} \{ ||v - \gamma(v)||_{\infty} \} \}$$

is the bottleneck distance between dgm(F) and dgm(F') where, for points a = (x,y) and $\gamma(a) = (x',y')$ in \mathbb{R}^2 , $||a-\gamma(a)||_{\infty} = \max\{|x-x'|,|y-y'|\}$ and $\gamma: dgm(F) \to dgm(F')$ is a bijection that can associate a point off the diagonal with another point on or off the diagonal. Here, diagonal is the set of points $\{(x,x)\}\subset\mathbb{R}^2$.

Remark 3 Since simplicial complexes considered in this paper are finite then for given filtrations F and F', we have that:

- dgm(F) is a finite set of points in \mathbb{R}^2 .
- $d_b(dgm(F), dgm(F')) = \min_{\gamma} \{ \max_a \{ ||a \gamma(a)||_{\infty} \} \}.$

In the following theorem, it is state that low-distortion correspondences between two PCDs, V and W, in \mathbb{R}^d give rise to small distance in the bottleneck distance of the persistence diagrams of the Čech filtrations \check{C}_V and \check{C}_W and the Vietoris-Rips filtrations VR_V and VR_W .

Theorem 4 Persistence stability for Čech and Vietoris-Rips complexes [14, Th. 5.2.] Let V and W be two sets of points in \mathbb{R}^d then, for either $F_V = \check{C}_V$ and $F_W = \check{C}_W$ or $F_V = VR_V$ and $F_W = VR_W$, we have that:

$$d_b(dgm(F_V), dgm(F_W)) \le 2d_{GH}(V, W),$$

where $2d_{GH}(V, W) = \inf_{c} \{ \sup_{v,v'} |d(v, v') - d(c(v), c(v'))| \} \}$ for $c: V \to W$ being surjective.

Remark 5 Since PCDs considered in this paper are finite, then

$$2d_{GH}(V,W) = \min_{c} \{ \max_{p,p'} |d(p,p') - d(c(p),c(p'))| \} \}.$$

6 Persistent entropy

In order to measure how much the construction of a filtration is ordered, a new entropy measure, the so-called *persistent entropy*, were defined in [6]. A precursor of this definition was given in [7] to measure how different the bars of a barcode were in length. In [8], persistent entropy was used for addressing the comparison between discrete piece-wise linear functions.

Definition 7 Given a filtration $F = \{K(t) | t \in \mathbb{R}\}$ and the corresponding persistence diagram $dgm(F) = \{a_i = (x_i, y_i) | 1 \le i \le n\}$ (being $x_i < y_i$ for all i), let $L = \{\ell_i = y_i - x_i | 1 \le i \le n\}$. The persistent entropy E(F) of F is calculated as follows:

$$E(F) = -\sum_{i=1}^{n} p_i \log(p_i)$$
 where $p_i = \frac{\ell_i}{S_L}$, $\ell_i = y_i - x_i$, and $S_L = \sum_{i=1}^{n} \ell_i$.

Sometimes, persistent entropy E(F) will also be denoted by E(L).

Note that the maximum persistent entropy would correspond to the situation in which all the bars in the associated persistence barcode are of equal length (i.e., $\ell_i = \ell_j$ for all $1 \le i, j \le n$). Conversely, the value of the persistent entropy decreases as more bars of different lengths are present in the persistence barcode. More concretely, if E(F) has n points, the possible values of E(F) lie in the interval $[0, \log(n)]$.

The following result supports the idea that persistent entropy can differentiate long from short bars as we will see in Section 15.

Theorem 8 [10] Given a filtration F and the corresponding persistence diagram $dgm(F) = \{a_i = (x_i, y_i) | 1 \le i \le n\}$, let $L = \{\ell_i = y_i - x_i | 1 \le i \le n\}$. For a fixed integer $i, 1 \le i \le n$, let

$$L' = \{\ell'_1, \dots, \ell'_i, \ell_{i+1}, \dots, \ell_n\}$$

where $\ell'_j = \frac{P_i}{e^{E(R_i)}}$ for $1 \le j \le i$, $R_i = \{\ell_{i+1}, \dots \ell_n\}$ and $P_i = \sum_{j=i+1}^n \ell_j$. Then

$$E(L) \leq E(L').$$

Observe that we can also write $\ell'_j = \prod_{j=i+1}^n \ell_j^{\ell_j/P_i}$. This last expression will be very useful in the proof of Th. 17 in Section 15.

Proof. Let us prove that E(L') is the maximum of all the possible persistent entropies associated to barcodes with n bars, such that the list of lengths of the last n-i bars of any of such lists is R_i . Let $M=\{x_1,\ldots,x_i,\ell_{i+1},\ldots,\ell_n\}$ (where $x_j>0$ for $1\leq j\leq i$) be any of such lists.

Let $S_x = \sum_{j=1}^i x_j$. Then, the persistent entropy associated to M is:

$$E(M) = -\sum_{j=1}^{i} \frac{x_j}{S_x + P_i} \log \left(\frac{x_j}{S_x + P_i} \right) - \sum_{j=i+1}^{n} \frac{\ell_j}{S_x + P_i} \log \left(\frac{\ell_j}{S_x + P_i} \right)$$

$$= -\sum_{i=1}^{i} \frac{x_j}{S_x + P_i} \log \left(\frac{x_j}{S_x + P_i} \right) - \frac{P_i E(R_i)}{S_x + P_i} - \frac{P_i}{S_x + P_i} \log \left(\frac{P_i}{S_x + P_i} \right).$$

In order to find out the maximum of E(M) with respect to the unknown variables x_k , $1 \le k \le i$, we compute the partial derivative of E(M) with respect to those variables:

$$\frac{\partial E(M)}{\partial x_k} = \frac{1}{(S_x + P_i)^2} \qquad \left(P_i E(R_i) + P_i \log \left(\frac{P_i}{x_k} \right) + \sum_{j \neq k} x_j \log \left(\frac{x_j}{x_k} \right) \right).$$

Finally, $\left\{x_k = \frac{P_i}{e^{E(R_i)}} \mid 1 \le k \le i\right\}$ is the solution of $\left\{\frac{\partial E(M)}{\partial x_k} = 0 \mid 1 \le k \le i\right\}$. \square The following result establishes a relation between bottleneck distance and

persistent entropy.

Proposition 9 Let F and F' be two filtrations. For all $\epsilon > 0$, there exists $\delta > 0$ such that if $d_b(dgm(F), dgm(F')) < \delta$ then $|E(F) - E(F')| < \epsilon$.

Proof. The proof is similar to the one given in [8] to demonstrate that persistent entropy associated to piece-wise linear functions is stable.

Fixed $\epsilon > 0$, we have to find $\delta > 0$ such that if $d_b(dqm(F), dqm(F')) < \delta$ then $|E(F) - E(F')| < \epsilon$.

First, since $h(x) = -x \log x$ is a continuous function in [0,1] (redefining h(0)as 0), for $\epsilon' = \frac{\epsilon}{n} > 0$, there exists $\delta' \in (0,1]$ such that if $|x - x'| \leq \delta'$ then $|h(x) - h'(x)| \leq \epsilon'$. Take $\delta = \frac{S_L \delta'}{4n}$ and suppose $d_b(dgm(F), dgm(F')) < \delta$. By Remark 3, dgm(F) and dgm(F') are both finite and there exists a bijection

 $\bar{\gamma}: dgm(F) \to dgm(F')$ such that $d_b(dgm(F), dgm(F')) = \max_a \{||a - \bar{\gamma}(a)||_{\infty}\}.$ Let $dgm(F) = \{a_1, \ldots, a_n\}$ (where some of the a_i can possibly be on the diagonal). Let $a_i = (x_i, y_i)$ and $\bar{\gamma}(a_i) = (x_i', y_i')$. Then,

$$||a_i - \bar{\gamma}(a_i)||_{\infty} = \max\{|x_i - x_i'|, |y_i - y_i'|\} \le \delta \text{ for all } i.$$

Let $\ell_i = y_i - x_i$ and $\ell'_i = y'_i - x'_i$. Then.

$$|\ell_i - \ell_i'| = |x_i - y_i - (x_i' - y_i')| \le |x_i - x_i'| + |y_i - y_i'| \le 2\delta$$
 for all i .

Besides.

$$|S_L - S_{L'}| = \left| \sum_{i=1}^n \ell_i - \sum_{i=1}^n \ell'_i \right| \le \sum_{i=1}^n |\ell_i - \ell'_i| \le 2\delta n.$$

Without lost of generality, assume $S_L \geq S_{L'}$. Then $S_L \leq S_{L'} + 2\delta n$. Let $p_i = \frac{\ell_i}{S_L}$ and $p_i' = \frac{\ell_i'}{S_{L'}}$. Then

$$p_i - p'_i = \frac{\ell_i}{S_L} - \frac{\ell'_i}{S_{L'}} = \frac{S_{L'}\ell_i - S_L\ell'_i}{S_L S_{L'}} \le \frac{\ell_i - \ell'_i}{S_{L'}} \le \frac{2\delta}{S_{L'}} = \frac{\delta'}{2n} \le \delta';$$

$$p_i' - p_i \leq \frac{(S_{L'} + 2\delta n)\ell_i' - S_{L'}\ell_i}{S_L S_{L'}} \leq \frac{\ell_i' - \ell_i}{S_{L'}} + \frac{2\delta n \ell_i'}{S_{L'} S_{L'}} \leq \frac{2\delta n}{S_{L'}} \left(1 + \frac{\ell_i'}{S_{L'}}\right) \leq \delta'.$$

Therefore,

$$|E(F) - E(F')| = \left| \sum_{i=1}^{n} p_i \log p_i - \sum_{i=1}^{n} p_i' \log p_i' \right| \le \sum_{i=1}^{n} |p_i \log p_i - p_i' \log p_i'| \le \epsilon,$$

which concludes the proof. \square The result above is used now to prove that persistent entropy is a stable measure for \dot{C} ech and Vietoris-Rips filtrations.

Theorem 10 Persistent entropy stability theorem for Čech and Vietoris-Rips filtrations. Let V and W be two PCDs in \mathbb{R}^d . Then, for every $\epsilon > 0$ there exists $\delta > 0$ such that:

If
$$2d_{GH}(V, W) \leq \delta$$
 then $|E(F_V) - E(F_W)| < \epsilon$,

where either $F_V = \check{C}_V$ and $F_W = \check{C}_W$ or $F_V = VR_V$ and $F_W = VR_W$.

Proof. First, by Prop. 9 we have that fixed $\epsilon > 0$, there exists $\delta > 0$ such that if $d_b(dgm(F_V), dgm(F_W)) < \delta$ then $|E(F_V) - E(F_W)| < \epsilon$. Second, by Th. 4 we have that $d_b(dgm(F_V), dgm(F_W)) \le 2d_{GH}(V, W)$. Therefore, if $2d_{GH}(V, W) < \delta$ then $|E(F_V) - E(F_W)| < \epsilon$.

11 Properties of the persistent entropy of Vietoris-Rips filtrations

Since Vietoris-Rips filtration are widely used in practice, we focus now our effort in the study of properties of the persistent entropy of this special kind of filtrations.

The first thing we have to take into account is that, in practice, one will never construct the filtration up to the end and will stop at a certain time T. Then, $VR_V = \{VR_V(t) | t \leq T\}$. To decide when to stop, we use the following result.

Proposition 12 Let $V = \{v_1, \ldots, v_m\}$ be a PCD in \mathbb{R}^d . Let

$$T = \frac{\min_{i} \max_{j} d(v_i, v_j)}{2}.$$

Then, $\beta_0(VR_V(T)) = 1$ and $\beta_k(VR_V(T)) = 0$ for k > 0.

Proof. First, notice that there exists a vertex v such that $\max_j d(v, v_j) = 2T$. That is, $d(v, v_j) \leq 2T$ for $1 \leq j \leq m$. Then, v is connected to v_j by an edge in $VR_V(T)$, for $1 \leq j \leq m$. In particular, $\beta_0(VR_V(T)) = 1$.

Now, observe that if $\sigma = \{v_0, v_1, \dots, v_k\}$ is a k-simplex in $VR_V(T)$ and $v \notin \sigma$, then $\sigma \cup \{v\} = \{v, v_0, v_1, \dots, v_k\}$ is a (k+1)-simplex in $VR_V(T)$ and $\partial_{k+1}(\sigma \cup \{v\}) = \sigma + \partial_k(\sigma) \cup \{v\}$.

Let $c = \sum_{i \in I} \sigma_i$ be a cycle in $C_k(VR_V(T))$. Let $J = \{j \mid j \in I \text{ and } v \text{ is not a vertex of } \sigma_j\}$. Let $b = \sum_{j \in J} \sigma_j \cup \{v\}$. Then

$$\partial_{k+1}(b) = \sum_{j \in J} \sigma_j + \partial_k(\sigma_j) \cup \{v\} = \sum_{j \in J} \sigma_j + \sum_{i \in I \setminus J} \sigma_i = c.$$

Therefore, c is a boundary. Then $\beta_k(VR_V(T)) = 0$ for k > 0. From now on, given a PCD $V = \{v_1, \dots, v_m\}$ in \mathbb{R}^d , we construct

$$VR_V = \{ VR_V(t) | t \le T \} \text{ for } T = \frac{\min_i \max_j d(v_i, v_j)}{2}.$$

By Prop. 12, the biggest bar in the persistence barcode in dimension 0 was born at time t = 0 and survives until the end (i.e., time t = T) and the smallest bar was born at time t = 0 and survives until $t = r = \min_{i,j} d(v_i, v_j)$. Fixed the number of bars in the persistence barcode and the maximum and minimum lengths of the bars, T and r, the following result shows the lengths of the rest of the bars that provide the minimum persistent entropy. This result will be very useful in the next section to detect topological features.

Theorem 13 Let $L = \{\ell_1, ..., \ell_n\}$ such that $\ell_1 = T$, $\ell_i \ge \ell_{i+1}$ for $1 \le i < n$ and $\ell_n = r$. Let $M = \{T, \stackrel{Q}{\dots}, T, r, \stackrel{n-Q}{\dots}, r\}$. Then

$$E(L) \ge E(M)$$
 for $Q = \left[\frac{\alpha n(\alpha - 1 - \log(\alpha))}{(\alpha - 1)^2}\right]$ being $\alpha = \frac{r}{T}$.

Proof. First, fixed n, T and r, Let $p_i = \frac{l_i}{S_L}$. Since the entropy is a concave function in

$$\Omega = \left\{ (p_1, p_2, \dots p_n) \mid \sum_{i=1}^n p_i = 1, \frac{1}{(n-1) + \alpha} < p_i < p_1 < \frac{1}{(n-1)\alpha + 1} \right\},\,$$

being $\alpha = \frac{r}{T}$, the minimum is attained at an extremal point of Ω . Let

$$P = (p_1, i_1, p_1, \alpha p_1, n_i, \alpha p_1), \text{ with } 1 < i < n,$$

be an extremal point. Since $\sum_{i=1}^{n} p_i = 1$, then $p_1 = \frac{1}{i + \alpha(n-i)}$ and the entropy of P is:

$$E(P) = \log(\alpha n) + \log(1 + \frac{i(1-\alpha)}{\alpha n}) - \frac{\log(\frac{1}{\alpha})}{1 + (\frac{n}{i} - 1)\alpha}.$$

Consider $t = \frac{i}{n} \in (0,1)$, then:

$$E(P) = E(t) = \frac{\alpha(1-t)\log(\frac{1}{\alpha})}{\alpha(1-t) + t}$$

The derivative of E(t) is null for:

$$t_0 = \frac{\alpha \log(\frac{1}{\alpha}) - \alpha(1 - \alpha)}{(1 - \alpha)^2}$$

So the minimum entropy is attained for

$$Q = [nt_0] = \left[n \frac{\alpha \log(\frac{1}{\alpha}) - \alpha(1 - \alpha)}{(1 - \alpha)^2} \right].$$

Taking in account that $p_1 = T$, the barcode with $l_1 = T$ and $l_n = r$ with minimum entropy is $M = \{T, \stackrel{Q}{\dots}, T, r, \stackrel{n-Q}{\dots}, r\}$.

In the following proposition, we establish the maximum entropy we can reach for n bars fixing the the maximum and minimum lengths of the bars.

Proposition 14 Fixed n, T and r, Let $L = \{\ell_1, \ldots, \ell_n\}$ such that $\ell_1 = T$, $\ell_i \geq \ell_{i+1}$ for $1 \leq i < n$ and $\ell_n = r$. Let

$$M' = \{T, b, \stackrel{n-2}{\dots}, b, r\}, \text{ where } b = T\alpha^{\alpha/(1+\alpha)} \text{ and } \alpha = \frac{r}{T}.$$

Then $E(L) \leq E(M')$.

Proof. First, reorder the list $L = \{\ell_2, \dots, \ell_n, \ell_1\}$ and then neutralize the bars ℓ_j for $2 \leq j \leq n-1$. By Th. 8, the new values that provide the maximum entropy are:

$$\ell'_j = T^{T/(r+T)} r^{r/(r+T)} = T^{1/(\alpha+1)} r^{\alpha/(\alpha+1)} = T \alpha^{\alpha/(\alpha+1)}.$$

Th. 13 and Prop. 14 confirm that the possible values of the persistent entropy B(F) of a filtration F associated to a PCD V is highly influenced by the number n of bars in B(F) and the rate between the minimum and maximum persistence entropy that we can reach with n bars. This rate is also influenced by the minimum distance r between two points in the PCD and the radius 2T of V. Now, given a persistence barcode L with n bars, maximum length of the bars equal to T and minimum length equal to r, the relative entropy E(L)/E(M'), being M' the possible maximum entropy with same data n, r and T, allows us to compare two persistence barcodes with different numbers of bars. Finally, observe that the value of Q in Th. 13 gives us a quantity of the maximum number of topological features we can find fixing the length of the persistence barcode and the maximum and minimum length of the bars.

15 Separating topological features from noise

Let us start now with a PCD $V = \{v_1, \ldots, v_m\}$ in \mathbb{R}^d from a distribution \mathbb{P} supported on a topological space \mathfrak{C} . Suppose the Vietoris-Rips filtration VR_V is computed from V (being $T = \frac{\min_i \max_j d(v_i, v_j)}{2}$), and the persistence barcode $B(VR_V)$ is computed from VR_V . The following are the steps of our proposed method, based on persistent entropy, to separate topological noise from topological features in the persistence barcode $B(VR_V)$, estimating, in this way, the topology of \mathfrak{C} .

Procedure 16 Computing topological features from the persistent barcode of the Vietoris-Rips filtration of a given PCD in \mathbb{R}^d .

Input: A $PCD V = \{v_1, ..., v_m\}$ in \mathbb{R}^d , its Vietoris-Rips filtration $VR_V = \{VR_V(t) | t \leq T\}$ and its associated persistence barcode $B(VR_V) = \{[x_i, y_i) | 1 \leq i \leq n\}$.

1. Sort the lengths of the bars in $B(VR_V)$ in decreasing order, except for the longest bar (whose length is equal to T) to obtain $L = \{\ell_1, \ldots, \ell_n\}$ such that $\ell_n = T \ge \ell_1$ and $\ell_i \le \ell_j \le \ell_{n-1} = r = \min_{i,j} d(v_i, v_j)$ for $1 \le i < j < n-1$.

Initially, $L'_0 := L$ and n' := n.

- 2. For i = 1 to i = n' 2 do:
 - a. Compute the persistent entropy $E(L_i')$ for $L_i' = \{\ell_1', \ldots, \ell_i', \ell_{i+1}, \ldots, \ell_{n'}\}$, being $\ell_j' = \frac{P_i'}{e^{E(R_i')}}$ for $1 \leq j \leq i$ as in Th. 8.
 - b. Compute

$$C = \frac{S_{L'_{i-1}}}{S_{L'_{i}}} = \frac{P'_{i-1} + (i-1)\frac{P'_{i-1}}{e^{E(R'_{i-1})}}}{P'_{i} + i\frac{P'_{i}}{e^{E(R'_{i})}}} \quad and \quad Q = \left[\frac{\alpha n'(\alpha - 1 - \log(\alpha))}{(\alpha - 1)^{2}}\right]$$

being $\alpha = \frac{r}{T}$.

while C > 1.

3. If Q < i, then the bars $[x_j, y_j)$ with i < j < n-1 represent noise in the pesistence barcode. Redefine $L'_0 := L'_0 \setminus \{\ell_{i+1}, \ldots, \ell_{n'-2}\}$ and n' := i+2. Go to step 2.

Else, the bars of $B(VR_V)$ with lengths in the set $\{T, \ell_1, \ldots, \ell_i\}$ represent topological features of VR_V .

• Output: The bars of $B(VR_V)$ that represent topological features of VR_V .

The following result guarantees the end of the while-loop in Proc. 16.

Theorem 17 Fixed n' in Proc. 16, there always exists a value $i, 1 \le i \le n'-2$, such that $C = \frac{S_{L'_{i-1}}}{S_{L'_{i}}} < 1$ except when T = r (which corresponds to a uniform distribution and, in this case, Q = n').

Proof. Observe that $L'_{n'-2} = \{b, \stackrel{n'-2}{\cdots} b, r, T\}$ for b as in Prop. 14. First, if $S_{L'_0} < S_{L'_{n'-2}}$ then:

$$\frac{S_{L'_0}}{S_{L'_{n'-2}}} = \frac{S_{L'_0}}{S_{L'_1}} \cdots \frac{S_{L'_{i-1}}}{S_{L'_i}} \cdots \frac{S_{L'_{n'-3}}}{S_{L'_{n'-2}}} < 1.$$

Then, there exists $i, 1 \leq i \leq n'-2$, such that $\frac{S_{L'_{i-1}}}{S_{L'_{i}}} < 1$.

Second, if $S_{L'_0} \geq S_{L'_{n'-2}}$, since $S_{L'_{n'-2}} = (n'-2)b + r + T$ then there exists i, $1 \leq i \leq n'-2$, such that $\ell_j \geq b$ for $j \leq i$ and $\ell_j < b$ for $i < j \leq n'-2$. Then, it is enough to prove that $S_{L'_i} < S_{L'_{n'-2}}$. By Th. 8, we have that:

$$S_{L_i'} = \sum_{j=1}^i \ell_i' + P_i' = i \prod_{j=i+1}^{n'} \ell_j^{\ell_j/P_i'} + P_i' = i \prod_{j=i+1}^{n'-2} \ell_j^{\ell_j/P_i'} T^{T/P_i'} r^{r/P_i'} + P_i'.$$

Observe that $P_i' < (n'-i-2)b+r+T$, since $\ell_j < b$ for $i < j \le n'-2$. Now, let us prove that

$$\prod_{i=i+1}^{n-2} \ell_j^{\ell_j/P_i'} T^{T/P_i'} r^{r/P_i'} < b,$$

which, taking the log of both sides, is equivalent to prove that:

$$\sum_{j=i+1}^{n'-2} \frac{\ell_j}{P_i'} \log(\ell_j) + \frac{T}{P_i'} \log(T) + \frac{r}{P_i'} \log(r) < \frac{T}{T+r} \log(T) + \frac{r}{T+r} \log(r).$$

Replacing P_i' by $\sum_{j=i+1}^{n'-2} \ell_j + r + T$ and simplifying, we have to prove that

$$\sum_{j=i+1}^{n'-2} \ell_j \log(\ell_j) < \frac{T \log(T) + r \log(r)}{T+r} \sum_{j=i+1}^{n'-2} \ell_j.$$

Since, for $i+1 \leq j \leq n'-2$, $\ell_j < b$, then $\log(\ell_j) < \frac{T \log(T) + r \log(r)}{T+r}$ which concludes the proof.

Observe that, in Proc. 16, for $1 \le i \le n'$, $E(L_i')$ is the entropy of the barcode obtained by replacing the first i bars of L_i' by i bars that maximize the entropy. Observe that $E(L_i') \le E(L_j')$ for $1 \le i < j \le n'$ by Th. 8. Then, the idea of the algorithm is to successively neutralize bars (using Th. 8) except for the longest and the shortest ones that are intrinsic in the nature of the filtration. We do it until $C = \frac{S_{L_{i-1}'}}{S_{L_i'}}$ is less than 1. What we measure with C is the change of the probability associated to the long bar [0,T) which, in step i, is $p_n^{(i)} = \frac{T}{S_{L_i'}}$. Observe that if a long bar is neutralize at step i, then $p_n^{(i-1)} \le p_n^{(i)}$, since neutralization in this case means to shorten the bar ℓ_i which produces an increase of the probability of the longest bar. On the other hand, if a short bar is neutralize at step i, then $p_n^{(i-1)} > p_n^{(i)}$, since neutralization in this case means to elongate the bar ℓ_i . In this last case, all the bars from ℓ_{i+1} to $\ell_{n'-2}$ are considered noise and removed from L_0' . We remove noise successively until the maximum number of topological features (computed as Q using Th. 13) is reached. Then, the algorithm ends.

Observe that this method is different from the one presented in [10]. In that paper, in order to appreciate the influence of the current length ℓ_i in the initial persistent entropy E(L), we divided $E(L'_i) - E(L'_{i-1})$ by $\log(n) - E(L)$ to obtain $H_{rel}(i)$. Then, we compare $H_{rel}(i)$ with $\frac{i}{n}$ since $H_{rel}(i)$ is affected by the total number of lengths and the number of lengths we are replacing. Nevertheless, the threshold $\frac{i}{n}$ was taken based on experimentation. In this paper, the constants C and Q and the thresholds C < 1 are founded on the mathematical results Th. 13, Prop. 14 and Th. 17.

We have applied our methodology to three different scenarios. First, we take 30 data points sampled from a circle of radius 1 (see Fig. 3.Left). This example has been taken from paper [9]. Vietoris-Rips complex for t=0.25 can be deduced from the picture shown in Fig. 3.Middle which consists of two connected components and zero loops. Looking at Vietoris-Rips complex for t=0.4 (see Fig. 3.Right), we assist at the birth and death of topological features: at t=0.4, one of the connected components has died (was merged with the other one), and a loop appears; this loop will die at t=1, when

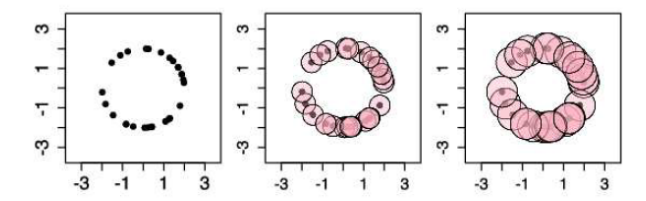


Figure 3: Left: 30 data points sampled from a circle of radius 1. Middle: Balls of radius 0.25 centered at the sample points. Right: Balls of radius 0.4 centered at the sample points.

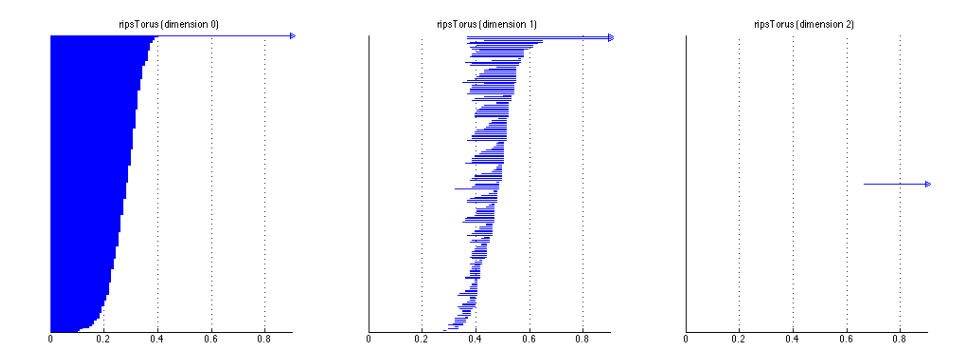


Figure 4: Barcodes (separated by dimension) computed from the Vietoris-Rips filtration associated to a point cloud lying on a 3D torus. Left: lifetimes of connected components. Middle: lifetimes of tunnels. Right: lifetimes of voids.

the union of the pink balls representing the distance function becomes simply connected. In Table 1.Top, we have applied our method to the bars that make up the persistence barcode (without differentiating dimension). This way, only the bars with length 1 (that corresponds to the connected component that survives until the end) and 0.6 (that correspond to the loop that appears at t=0.4 and disappears at t=1) are considered topological features. Later, in Table 1.Bottom, we have applied our method to the bars that make up the persistence 0-barcode (i.e., the lifetime of the connected components along the filtration). This way, the bars with length 1 and 0.35 (that corresponds to the connected components that dies just before the loop is created) are considered topological features.

Second, consider now a set V of 400 points sampled from a 3D torus. The barcodes (separated by dimension) computed from the Vietoris-Rips filtration associated to V are showed in Fig. 4. We have applied our method to the 0-barcode (lifetime of connected components along the V-R filtration) and the 1-barcode (lifetime of loops along the V-R filtration). See Table 2. The bar of length 1.9 in the tables corresponds to the connected component that survives until the end. The bars of length 1.531 correspond to the two tunnels of the

Iteration	n'	Q	E(L')/E(M')	α
1	30	5	0.93451	0.05
ℓ_i	ℓ_i'	С	$E(L_i')/E(M')$	Feature?
1.	0.0412134	1.06692	0.944278	yes
0.6	0.0409925	1.0259	0.945869	yes
0.35	0.0409923	1.00065	0.945870	yes
0.225	0.0409921	1.00071	0.945872	yes
0.225	0.0409835	0.995049	0.945934	yes
0.2	0.0409741	0.99457	0.946002	no
0.2	0.0409637	0.994018	0.946077	no

Iteration	n'	Q	E(L')/E(M')	α
2	6	1	0.917626	0.05
ℓ_i	ℓ_i'	С	$E(L_i')/E(M')$	Feature?
1.	0.2165	1.03422	0.918784	yes
0.6	0.213219	0.900062	0.927951	yes
0.35	0.20185	0.806752	0.960854	no
0.225	0.18911	0.746703	1.	no

Table 1: Results of our method applied to the barcode obtained from the PCD showed in Fig. 3 consisting of 30 data points sampled from a circle of radius 1.

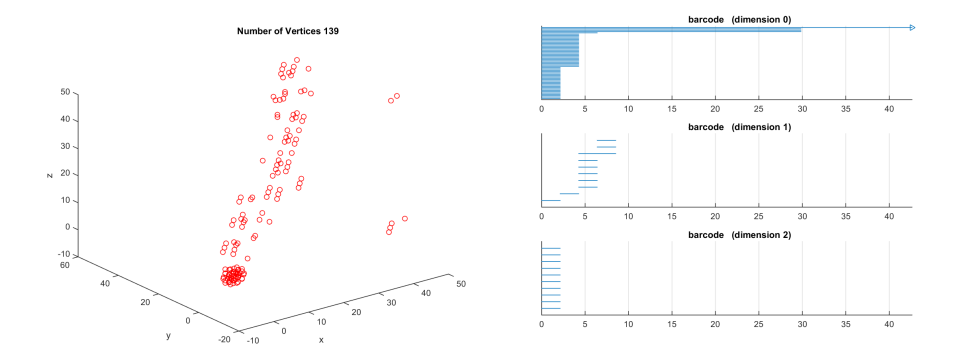


Figure 5: Left: A PCD V in \mathbb{R}^3 composed by 139 points. Right, from top to bottom: 0-, 1- and 2-dimensional persistence barcode of VR_V .

3D torus. In Table 2.Bottom we show the results of our method applied to all the bars of the persistence barcode without separating by dimensions. We can see in this case that we obtain as topological features the length of the bar representing the connected component, the ones representing the two tunnels and the one representing the void. In Table 2.Top (resp. Table 2.Middle), we show the results of our method applied to the bars of the 0-dimensional (resp. 1-dimensional) persistence barcode. Observe that the results are consistent with the ones obtained in Table 2.Bottom.

Finally, consider a PCD V of 76 points in \mathbb{R}^3 . The barcodes (separated by dimension) computed from the Vietoris-Rips filtration associated to V are showed in Fig. 5.Right. In Table 3.Top, we have applied our method to the 0-barcode and in Table 3.Bottom, the method is applied to all the bars of the barcode without differentiating by dimension. We can see that in both cases we obtain 5 topological features. The idea is that, compared to the longest bars in the 0-barcode, the bars in the 1- and 2-barcodes are considered noise: The two tunnels and the one representing the void. This example shows that, since bars in higher dimensions than 0 are noise, the results obtained with our method are independent on applying it on the whole set of bars of the persistence barcode or separating the bars by dimension.

18 Conclusions and future work

Vietoris-Rips complexes are a fundamental tool in topological data analysis, they allow to build a topological space from higher dimensional data-set embedded in a metric space [15]. The resulting complex is then studied by persistent homology. In order to provide a summary of the information provided by persistent homology new statistics have been defined. Among the statistics, we put our focus on a Shannon-like entropy that is known as persistent entropy. Persistent entropy records how much is ordered the construction of a topological space.

Iteration	n'	Q	E(L')/E(M')	α
1	400	47	0.993675	0.0521053
2	286	34	0.995459	0.0521053
3	154	19	0.993659	0.0521053
4	40	5	0.977194	0.0521053
ℓ_i	ℓ_i'	С	$E(L_i')/E(M')$	Feature?
1.9	0.0270463	0.997193	0.977234	yes
0.396	0.0270402	0.996476	0.977294	no
0.387	0.0270339	0.996296	0.977357	no

Iteration	n'	Q	E(L')/E(M')	α
1	177	5	0.893511	0.00587851
2	50	2	0.904135	0.00587851
3	6	1	0.796461	0.00587851
ℓ_i	ℓ_i'	С	$E(L_i')/E(M')$	Feature?
1.531	0.264348	1.22428	0.822957	yes
1.531	0.242872	0.791795	0.875366	yes
0.27	0.221058	0.751341	0.933577	no
0.261	0.198549	0.703848	1.	no

Iteration	n'	Q	E(L')/E(M')	α
1	578	47	0.969019	0.00473684
2	429	9	0.988556	0.00473684
3	306	7	0.989757	0.00473684
4	179	4	0.985682	0.00473684
5	43	1	0.95329	0.00473684
ℓ_i	ℓ_i'	С	$E(L_i')/E(M')$	Feature?
1.9	0.0268932	1.05166	0.961183	yes
1.531	0.0259429	1.05987	0.970746	yes
1.531	0.0253107	1.04887	0.977304	yes
1.234	0.0253068	0.996996	0.977345	yes
0.396	0.025301	0.99627	0.977407	no
0.387	0.0252948	0.996079	0.977471	no

Table 2: Results of our method applied to the persistence barcodes of the Vietoris-Rips filtration obtained from 400 points sampled from a 3D torus. In the table on the top, only bars in the 0-dimensional pesistence barcode are taken into account. In the table on the middle, only bars in the 1-dimensional pesistence barcode are considered. In the table on the bottom, the bars of persistence barcodes of dimension 0, 1 and 2 are considered altogether.

Iteration	n'	Q	E(L')/E(M')	α
1	76	9	0.857307	0.05
ℓ_i	ℓ_i'	С	$E(L_i')/E(M')$	Feature?
42.4484	0.023405	1.06815	0.869108	yes
31.8363	0.0219565	1.08028	0.883896	yes
31.8363	0.0202248	1.09583	0.902912	yes
31.8363	0.0181347	1.11616	0.928160	yes
31.8363	0.0181326	0.997812	0.928187	yes
4.24484	0.0181304	0.997733	0.928215	no
4.24484	0.0181281	0.99765	0.928244	no

Iteration	n'	Q	E(L')/E(M')	α
1	98	12	0.870766	0.05
2	30	4	0.852821	0.05
ℓ_i	ℓ_i'	С	$E(L_i')/E(M')$	Feature?
42.4484	0.023405	1.06815	0.861170	yes
31.8363	0.0219565	1.08028	0.8725486	yes
31.8363	0.0202248	1.09583	0.888921	yes
31.8363	0.0181347	1.11616	0.914344	yes
31.8363	0.0181326	0.997812	0.916294	yes
4.24484	0.0181304	0.997733	0.918325	no
4.24484	0.0181281	0.99765	0.920440	no

Table 3: Results of our method applied to the PCD showed in Fig. 5.

In this paper, we discuss several properties of the persistent entropy when it is computed on the persistence barcode of a given Vietoris-Rips filtration. The first property demonstrates the relations between persistent entropy and the bottleneck distance, that is a well known measures for comparing persistence barcodes. This is a preliminary results for assuring that persistent entropy is a stable measure for dealing with Vietoris-Rips complexes. Moreover, the computation of persistent entropy is less computational expensive with respect to the bottleneck distance. Because the construction of Vietoris-Rips depends on the choice of the upper bound of a parameter, we identify a new quantity that can be used for and we hope this can be a signpost by the reader when he/she starts to investigate the construction of the Vietoris-Rips complexes. By introducing this quantity we are able to define a new methodology based on persistent entropy for identifying which are true topological features and which must be considered noisy topological features. We apply the methodology on a couple of examples. Briefly, the method is an iterative algorithm that at the i-th step replaces the first i bars by the same number of bars but with the length that maximizes the entropy. This way we "neutralize" the effect of such i bars and we can deduce if the bar at position i is a topological feature or not.

As future works we are planning to extend the properties to the Witness complexes, that are roughly speaking a way for computing the Vietoris-Rips complexes from very large data-set. This will allow us to use our method for studying biological data as well as RNA data for differentiating healthy cells from unhealthy cells [16, 17]. We argue the method will let to highlight the topological features that are formed by the most relevant genes associated to pathologies.

References

- [1] J. Binchi, E. Merelli, M. Rucco, G. Petri, F. Vaccarino, jholes: A tool for understanding biological complex networks via clique weight rank persistent homology, Electronic Notes in Theoretical Computer Science 306 (2014) 5–18.
- [2] H. Adams, A. Tausz, Javaplex tutorial (2011).
- [3] A. Mamuye, E. Merelli, M. Rucco, Persistent homology analysis of the rna folding space, in: Proc. 9th EAI Conference on Bio-inspired Information and Communications Technologies (BICT 2015), 2015.
- [4] N. Jonoska, M. Saito, Discrete and Topological Models in Molecular Biology, Springer, 2013.
- [5] P. Bubenik, Statistical topological data analysis using persistence land-scapes, The Journal of Machine Learning Research 16 (1) (2015) 77–102.
- [6] M. Rucco, F. Castiglione, E. Merelli, M. Pettini, Characterisation of the idiotypic immune network through persistent entropy, in: Proc. Complex, 2015.

- [7] H. Chintakunta, T. Gentimis, R. Gonzalez-Diaz, M. J. Jimenez, H. Krim, An entropybased persistence barcode, Pattern Recognition 48 (2) (2015) 391–401.
- [8] M. Rucco, R. Gonzalez-Diaz, M. J. Jimenez, N. Atienza, C. Cristalli, E. Concettoni, A. Ferrante, E. Merelli, A new topological entropy-based approach for measuring similarities among piecewise linear functions, Signal Processing 134 (2017) 130 138. doi:http://dx.doi.org/10.1016/j.sigpro.2016.12.006. URL http://www.sciencedirect.com/science/article/pii/S0165168416303486
- [9] B. T. Fasy, F. Lecci, A. Rinaldo, L. Wasserman, S. Balakrishnan, A. Singh, Confidence sets for persistence diagrams, The Annals of Statistics 6 (2014) 2301–2339.
- [10] N. Atienza, R. Gonzalez-Diaz, M. Rucco, Separating topological noise from features using persistent entropy, in: Software Technologies: Applications and Foundations STAF 2016 Collocated Workshops: DataMod, GCM, HOFM, MELO, SEMS, VeryComp, Vienna, Austria, July 4-8, 2016, Revised Selected Papers, 2016, pp. 3–12. doi:10.1007/9783-319-50230-4 1. URL http://dx.doi.org/10.1007/978-3-319-50230-4 1
- [11] H. Edelsbrunner, J. Harer, Computational topology: an introduction, American Mathematical Soc., 2010.
- [12] A. Hatcher, Algebraic topology. Cambridge university press, Cambridge, UK.
- [13] J. R. Munkres, Elements of algebraic topology, Vol. 2, Addison-Wesley,
- [14] F. Chazal, V. de Silva, S. Oudot, Persistence stability for geometric complexes, Geometriae Dedicata 173 (1) (2014) 193–214. doi:10.1007/s10711-013-9937-z. URL http://dx.doi.org/10.1007/s10711-013-9937-z
- [15] V. Nanda, R. Sazdanovic, Simplicial models and topological inference in biological systems, in: Discrete and Topological Models in Molecular Biology, Springer, 2014, pp. 109–141.
- [16] K. Davie, J. Jacobs, M. Atkins, D. Potier, V. Christiaens, G. Halder, S. Aerts, Discovery of transcription factors and regulatory regions driving in vivo tumor development by atac-seq and faire-seq open chromatin profiling, PLoS Genet 11 (2) (2015) e1004994.
- [17] C. Nasuti, S. Ferraro, R. Giovannetti, M. Piangerelli, R. Gabbianelli, Metal and microelement biomarkers of neurodegeneration in early life permethrintreated rats, Toxics 4 (1) (2016) 3.